

A CLOUD-BASED URBAN MONITORING SYSTEM BY USING A QUADCOPTER AND INTELLIGENT LEARNING TECHNIQUES

Submitted: 21st December 2021; accepted 24th February 2022

Sohrab Khanmohammadi, Mohammad Samadi

DOI: 10.14313/JAMRIS/2-2022/11

Abstract:

The application of quadcopter and intelligent learning techniques in urban monitoring systems can improve flexibility and efficiency features. This paper proposes a cloud-based urban monitoring system that uses deep learning, fuzzy system, image processing, pattern recognition, and Bayesian network. The main objectives of this system are to monitor climate status, temperature, humidity, and smoke, as well as to detect fire occurrences based on the above intelligent techniques. The quadcopter transmits sensing data of the temperature, humidity, and smoke sensors, geographical coordinates, image frames, and videos to a control station via RF communications. In the control station side, the monitoring capabilities are designed by graphical tools to show urban areas with RGB colors according to the predetermined data ranges. The evaluation process illustrates simulation results of the deep neural network applied to climate status and effects of the sensors' data changes on climate status. An illustrative example is used to draw the simulated area using RGB colors. Furthermore, circuit of the quadcopter side is designed using electric devices.

Keywords: *urban monitoring, cloud computing, quadcopter, deep learning, fuzzy system, image processing, pattern recognition, bayesian network, intelligent techniques, learning systems*

1. Introduction

Urban monitoring systems are essential application tools in today's world. A wide range of urban monitoring applications is evident proof of growing interest in this field. These systems can be designed and implemented by using various electromechanical devices such as sensors, off-the-shelf cameras, and microphones. For example, available parking can be tracked in a metropolitan area and urban traffic can be controlled by monitoring tools. Existing urban monitoring solutions are primarily composed of static sensor deployment and pre-defined communication/software infrastructures. Therefore, they are hardly scalable and are vulnerable when conducting their assigned purposes [1–3].

A quadcopter – namely multirotor, quadrotor, or drone – is a simple flying electromechanical vehicle

that is composed of four arms and a motor attached to the propeller on each arm. Two rotors turn clockwise, and the other two turn counterclockwise. A flight computer or controller can be applied to convert the operator's commands into the desired motion. Quadcopters can be equipped with various electromechanical devices (e.g., sensor and camera) to gather the data on phenomena in urban areas [4–6].

Quadcopters transmit big data to the monitoring servers. These big data should be stored as a database so various results can be derived according to the reported information. Cloud computing offers the main support for targeting the primary challenges with shared computing resources (e.g., computing, storage, and networking). The application of these computing resources has performed impressive big data advancements [7–10].

Most existing urban monitoring systems [21–24] consist of stationary devices on urban fields. This feature inhibits system flexibility, and operational costs are noticeably enhanced. The application of a quadcopter with the aid of cloud computing, image processing [11], and intelligent learning systems (such as deep learning [12, 13], deep neural network [14], fuzzy decision making [15–18], pattern recognition [19], and Bayesian network [20]), can considerably improve the efficiency of existing monitoring systems. A cloud-based urban monitoring system is proposed in this paper based on using a quadcopter and intelligent learning systems. It uses sensing data of the temperature, humidity, and smoke sensors to determine climate status via deep learning. The system uses geographic coordinates and sensing data to conduct the climate, temperature, humidity, and smoke monitoring using fuzzy systems, image processing, and RGB colors. Pattern recognition and Bayesian networks are also applied to detect fire occurrence over urban areas. It seems that the proposed system can improve the existing urban monitoring systems.

Section 2 represents a literature review of the existing urban monitoring systems. Section 3 describes units and strategies of the proposed cloud-based urban monitoring system. Section 4 evaluates the proposed deep learning unit, monitoring tools, and the detection of fire occurrence. Section 5 provides circuit design of the quadcopter side by using electric devices. Finally, the paper is concluded in Section 6.

2. Literature Review

Calabrese et al. [21] have described a real-time urban monitoring system using the Localizing and Handling Network Event Systems (LoCHNESs) platform. The system is designed by Telecom Italia for the real-time analysis of urban dynamics according to the anonymous monitoring of mobile cellular networks. The instantaneous positioning of buses and taxis is utilized to give information about urban mobility in real-time situations. This system can be used for monitoring a variety of phenomena in different regions of cities, from traffic conditions to the movements of pedestrians.

Abraham and Pandian [22] have presented a low-cost mobile urban environmental monitoring system based on off-the-shelf open-source hardware and software. They have developed the system in such a way that it can be installed or applied in public transport vehicles, especially in the school and college buses in various countries (e.g., India). Moreover, a pollution map of the local and regional areas can be provided from the gathered data in order to enhance the awareness of urban pollution problems.

Lee et al. [23] have applied wireless sensor networks, Bluetooth sensors, and Zigbee transceivers to provide a low-cost and energy-saving urban mobility monitoring system. The Bluetooth sensor captures MAC addresses of the Bluetooth units which are equipped in car navigation systems and mobile devices. The Zigbee transceiver then transmits the gathered MAC addresses to a data center without using any fundamental communication infrastructures (e.g., 3G/4G networks).

Shaban et al. [24] have presented a monitoring and forecasting system for urban air pollution. This system applies the low-cost, air-quality monitoring motes which are equipped with gaseous and meteorological sensors. The modules receive and then store the data, convert the data into useful information, predict the pollutants with historical information, and finally address the collected information via various channels (e.g., mobile application). Moreover, three machine learning algorithms are utilized to construct accurate forecasting models.

3. The Proposed Cloud-Based Urban Monitoring System

The proposed monitoring system provides various monitoring features including climate, temperature, humidity, and smoke monitors, and the detection of fire occurrence. First, a quadcopter – flying over urban areas – transmits temperature, humidity, smoke, geographical coordinates, image, and video data toward a control station in a specified period of time. Then, the control station conducts the above monitoring features by using deep learning, fuzzy systems, image processing, pattern recognition, and Bayesian networks based on the data transmitted from the quadcopter. It uses a software framework via graphical tools to manage tasks created by the monitoring

purposes. This section describes units and strategies of this system.

3.1. System Model

In the supposed model, a quadcopter flies over urban areas based on the flight control system presented by Zhao and Go [25] in order to gather various phenomenal data including temperature, humidity, smoke, geographical coordinates, images, and videos. The quadcopter is equipped with different sensors and electromechanical devices such as temperature sensor, Global Positioning System (GPS), and camera. It transmits the sensed data toward a control station (e.g., a laptop) via RF communications in a specified period of time. The control station stores the received data in a MongoDB cloud database. Upon receiving the data from the quadcopter, it calculates the climate status, monitors four environmental conditions by graphical tools, and detects fire occurrence based on the phenomena data. The sensing data range of temperature sensor is (0, 80) °C, humidity sensor is (0, 100) % RH, and smoke sensor is (10, 10000) ppm. Note that some of the temperature sensors sense a heat data below 0 °C and/or higher than 80 °C. Thus, the system model only considers the sensing data in the range of (0, 80) °C. Fig. 1 represents the schematic model of the proposed monitoring system.

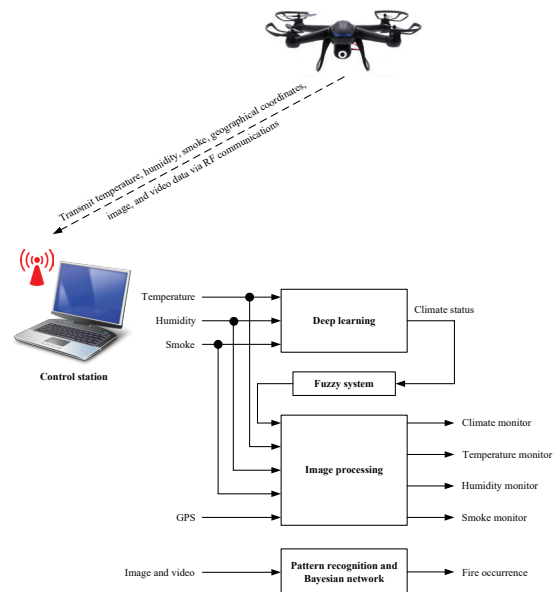


Fig. 1. Schematic model of the proposed monitoring system

3.2. Calculation of the Climate Status by Deep Learning

Deep neural network [26, 27] can give a deep learning feature to the proposed system. It leads to the climate status to be determined precisely based on the input data. In this unit, temperature, humidity, and smoke are the input data, while climate status is the output data. Fig. 2 illustrates a deep neural network to calculate quantitative value of the climate status in the range of (0, 100) %. Each neuron uses a Perceptron function [28] to transmit an appropriate value to the next layer based on the values received from previous layer, as below

$$F = \sum_{i=1}^n x_i w_i + b \tag{1}$$

where n is number of neurons and b is bias. The weights between neurons at the subsequent layers are determined in the network based on experimental results and human experiences.

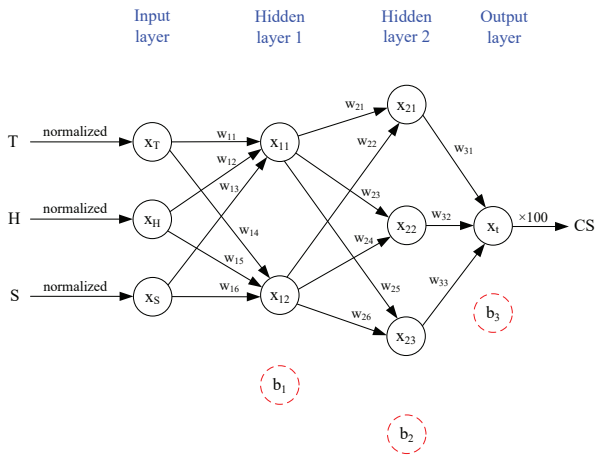


Fig. 2. Schematic of a deep neural network to calculate climate status

The value of climate status can be calculated as follows

$$CS = x_r \times 100 = (x_{21} w_{31} + x_{22} w_{32} + x_{23} w_{33} + b_3) \times 100$$

where w_{ij} s are determined after the learning process of the neural network.

Note that the normalized value of each neuron at the input layer can be determined as

$$x_T = \frac{T}{Max_T}, x_H = \frac{H}{Max_H}, x_S = \frac{S}{Max_S}$$

Consequently, climate status is calculated as

$$CS = (w_{31} \frac{T}{Max_T} + w_{32} \frac{H}{Max_H} + w_{33} \frac{S}{Max_S} + b_3) \times 100 \tag{2}$$

where T is temperature data, Max_T is the maximum sensing data of the temperature sensor, H is humidity data, Max_H is the maximum sensing data of the humidity sensor, S is smoke data, Max_S is the maximum sensing data of the smoke sensor, w_{ij} s are the weights of output layer; and b_3 is the bias value. As represented in the above calculations, quantitative amounts of the weights and biases are defined in a way that the complexity of all equations is reduced noticeably. If climate status is low then environmental condition is favorable; otherwise, environmental condition is critical.

3.3. Monitoring Tools Using Fuzzy System and Image Processing

Monitoring system consists of four monitoring tools: climate monitor, temperature monitor, hu-

midity monitor, and smoke monitor. Monitoring results are carried out based on data transmissions of the quadcopter and geographical coordinates. Climate monitor is illustrated for various regions on the urban areas, while the other monitors are done for each point on the areas via a point-to-point process.

Climate monitors are an essential monitoring tool in urban management systems. It can depict climate conditions of all locations. The climate monitor of the proposed system is conducted for various regions on the map. That is, the whole map is categorized into various regions so that each region has a unique climate status. First, a unique status is determined for each region by a proposed fuzzy system. Then, every region will be shown by an RGB color, based on the unique climate status through an image processing phase. Note that the dimensions of every region – in this system – are considered to be 100×100 points. The input variables of the fuzzy system are “Number of repeats” and “Distance to mean.” The output variable of the system is “Selection rate” as illustrated in Fig. 3. Universe of discourse for “Number of repeats” and “Distance to mean” is {0, 2500, 5000, 7500, 10000}, while universe of discourse for “Selection rate” is {0, 25, 50, 75, 100}. Linguistic terms of “Number of repeats” are {“Few”, “Normal”, “Many”}, linguistic terms of “Distance to mean” are {“Near”, “Mediocre”, “Far”}, and linguistic terms of “Selection rate” are {“Low”, “Medium”, “High”}. Membership functions of the inputs are determined by the triangular function and membership functions of the output are specified by the bell-shaped function [29]. Moreover, rule-making process is performed by the Mamdani-type fuzzy system [30]. Table 1 represents IF-THEN rules of the fuzzy system.

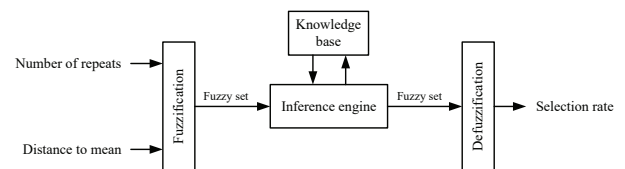


Fig. 3. Main elements of the proposed fuzzy system

Table 1. IF-THEN fuzzy rules of the proposed fuzzy system

Rule #	Input variables		Output variable
	Number of repeats	Distance to mean	Selection rate
1	Few	Near	Medium
2	Few	Mediocre	Low
3	Few	Far	Low
4	Normal	Near	Medium
5	Normal	Mediocre	Medium
6	Normal	Far	Low
7	Many	Near	High
8	Many	Mediocre	High
9	Many	Far	Medium

Fuzzification

Fuzzification converts real numbers as well as linguistic terms to fuzzy sets. That is, it specifies *MFs* of the inputs and the output. The triangular function is calculated as below:

$$\text{triangular}(x; a, m, b) = \begin{cases} 0 & x \leq a \\ (x-a)/(m-a) & a < x \leq m \\ (b-x)/(b-m) & m < x < b \\ 0 & x \geq b \end{cases} \quad (3)$$

where x indicates a member of the universe of discourse, a represents the lower limit, b indicates the upper limit, and m represents the center of triangle. The bell-shaped function is determined as following

$$\text{bell shapd}(x; a, b, c) = \frac{1}{1 + \left| \frac{x-c}{a} \right|^{2b}} \quad (4)$$

where x indicates a member of the universe of discourse, c and a adjust the center and width of the membership function, and b represents the slope at the cross points.

Rule Base

The relation between the inputs and the output in the proposed fuzzy system is expressed in terms of a set of the IF-THEN fuzzy rules listed in Table 1.

Inference Engine

As mentioned before, the inference engine in the proposed fuzzy system applies the Mamdani-type system. It performs based on the given rule base as follows:

$$\begin{aligned} C' &= (A' \times B') \circ R \\ &= (A' \times B') \circ \left(\bigcup_{j=1}^m R_j \right) \\ &= (A' \times B') \circ \left(\bigcup_{j=1}^m (A_j \times B_j \times C_j) \right) \end{aligned} \quad (5)$$

where A_j , B_j , and C_j indicate the *MFs* of the inputs and the output applied in the fuzzy rules, R represents the total rule of the fuzzy rules, R_j indicates a fuzzy rule in the rule base, m represents the number of fuzzy rules, A' and B' indicate the membership grades of two inputs fed from the input parameters, and C' represents the membership grade of the output determined based on the inputs' values.

Defuzzification

The center-of-gravity method is used to specify crisp value of a fuzzy output, as below

$$T(n) = \frac{\sum_{i=1}^p \mu_T(x_i) * x_i}{\sum_{i=1}^p \mu_T(x_i)} \quad (6)$$

where x_i is a member of the output universe of discourse, $\mu_T(x_i)$ is the membership degree of x_i , and p is the number of members in the output universe of discourse [31–37].

Algorithm 1 represents how to select an appropriate climate status for each region. Lines 1 to 4 define initial variables of the procedure. Line 8 calculates average climate status of each region based on the values of CS. Line 9 determines number of repeats and line 10 determines distance to mean of all climate statuses at current region in the range of [0, 100]. Afterward, line 11 calculates success rate of the climate statuses using the fuzzy system. Finally, lines 12 to 14 select an appropriate climate status, set the statuses of all points to the selected status, and depict the whole region by an RGB color based on the selected climate status.

Table 2 indicates four RGB colors that are determined for climate statuses. These colors are used to illustrate all regions via image processing. All climate statuses are categorized into four terms to draw regions with an appropriate RGB color based on the selected status.

Temperature, humidity, and smoke monitors are other tools in the proposed monitoring system that will be conducted based on sensing data of the quadcopter's sensors. They are managed by a point-to-point process to draw each point on the map by image processing techniques. Table 3 represents how to select an appropriate RGB color for every point based on sensing data of the temperature, humidity, and smoke sensors.

Algorithm 1. Climate monitor of the urban areas	
1:	L ← Length of the area
2:	W ← Width of the area
3:	CS[1..L][1..W] ← Climate status of all the points
4:	i ← 1
5:	While (i < L){
6:	j ← 1
7:	While (j < W){
8:	Avg ← Average climate status of the CS[i..i+99][j..j+99]
9:	NR[1..100] ← Number of repeats
10:	DM[1..100] ← Distance to mean
11:	SR[1..100] ← Success rate
12:	Select the climate status with the most success rate
13:	Set all points of current region to the selected status
14:	Depict the region by the RGB color associated to the selected status
15:	j ← j + 100
16:	}
17:	i ← i + 100
18:	}

3.4. Detection of Fire Occurrence via Pattern Recognition and Bayesian Network

The proposed system applies the fire detection algorithm presented by Ko et al. [38] by using irregular

patterns of flames and hierarchical Bayesian network. Fig. 4 shows various elements and steps of this detection algorithm. The overall system is divided to two main steps: pre-processing step and fire verification step. In the pre-processing step, input image is analyzed after using the adaptive background subtraction and color probability models. The image can be obtained based on the image and/or video data transmitted from the quadcopter.

Table 2. RGB color of the selected climate status in climate monitor












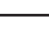



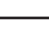
Climate status (%)	Climate term	Color	RGB color
[0..20]	Excellent		RGB(78, 97, 40)
[21..50]	Good		RGB(118, 146, 60)
[51..80]	Critical		RGB(194, 214, 155)
[81..100]	Emergency		RGB(214, 227, 188)

Table 3. RGB color of sensing data in the temperature, humidity, and smoke monitors

Type	Sensing data	Term	Color	RGB color
Temperature monitor	[0..5] °C	Cold		RGB (192, 0, 0)
	[6..20] °C	Cool		RGB (255, 0, 0)
	[21..35] °C	Moderate		RGB (255, 101, 101)
	[36..80] °C	Hot		RGB (255, 175, 175)
Humidity monitor	[0..15] % RH	Dry		RGB (0, 0, 164)
	[16..40] % RH	Medium		RGB (0, 0, 255)
	[41..70] % RH	Wet		RGB (71, 71, 255)
	[71..100] % RH	Very wet		RGB (139, 139, 255)
Smoke monitor	[10..1000] ppm	Low density		RGB (0, 0, 0)
	[1001..3000] ppm	Normal		RGB (64, 64, 64)
	[3001..6000] ppm	Noticeable		RGB (128, 128, 128)
	[6001..10000] ppm	High density		RGB (180, 180, 180)

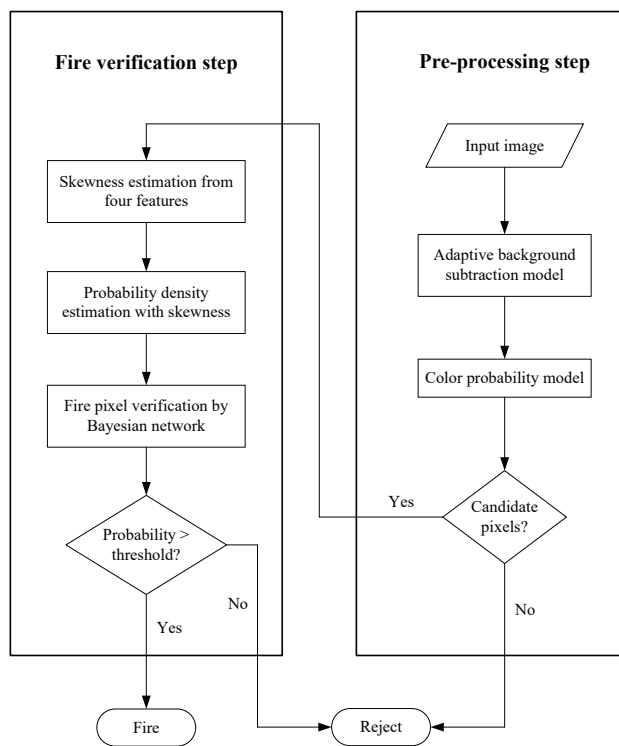


Fig. 4. A work flow for the detection algorithm of fire occurrence by pattern recognition and Bayesian network [38]

Afterward, if pixels are selected in the candidate process then they will be forwarded to the next step; otherwise, the current process of system will be terminated. In the fire verification step, skewness estimation uses four fire features to evaluate the pixels of input image. Then, probability density is estimated by skewness, and fire pixels are verified by a Bayesian network. If the probability is greater than a predefined threshold value then the fire occurrence will be detected; otherwise, the analysis process will be rejected.

4. Evaluation Results

This section evaluates the efficiency of some units that are considered in the proposed monitoring system, including deep learning, monitors, as well as pattern recognition and Bayesian networks. Simulation results are carried out according to the proposed system model. However, some of the simulation parameters are changed in some cases to demonstrate the difference between various scenarios.

Fig. 5 shows an instance of the simulation results for the proposed deep neural network. The results are carried out in 2500 points for the temperature, humidity, and smoke sensors. Moreover, climate status is calculated for these points based on sensing data of the sensors. It is evident that, in most of the points, climate status is critical because the temperature, humidity, and smoke data are high.

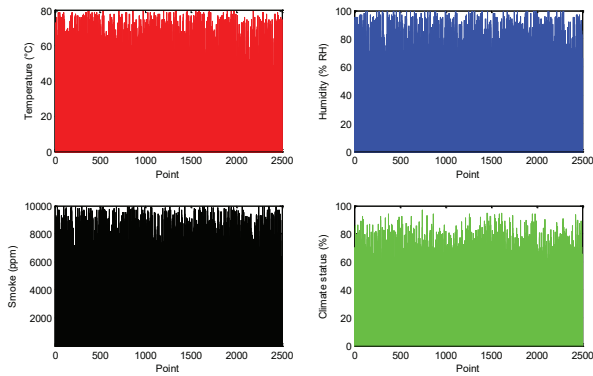


Fig. 5. Simulation results of the deep neural network in the deep learning unit

Fig. 6 illustrates effects of the temperature, humidity, and smoke changes on climate status in the deep learning unit. Default values of the temperature, humidity, and smoke sensors are considered to be equal to 30 °C, 50% RH, and 4000 ppm, respectively. As indicated by the simulation results, these changes are harmonic for all the sensors. The reason is that effects of the temperature, humidity, and smoke sensors on climate status are linear. Since the default values of sensors are not supposed very low, the minimum climate status is 25.

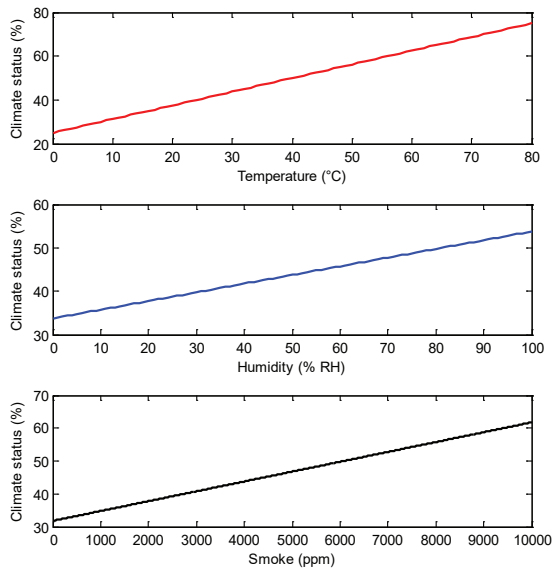


Fig. 6. Effects of the temperature, humidity, and smoke changes on climate status

Fig. 7 illustrates an example of the simulation results that are carried out by the temperature, humidity, and smoke monitors. The simulation process is conducted in an urban area with the dimensions of 1500 × 500 points. It considers only 20 instances of the temperature, humidity, and smoke data that are transmitted from the quadcopter and then are stored in the MongoDB database. Each instance is painted by a RGB color, according to the descriptions in Table 3.

In most cases, simulation results indicate that temperature is hot, humidity is medium, and smoke has high density.

As represented before, the pattern recognition and Bayesian network unit uses a file detection algorithm that is presented by Ko et al. [38]. This work is compared to Töreyn’s method [39] and Ko’s method [40] in terms of true positive and detection speed, as indicated by Table 4. Comparison results demonstrate that, in most video sequences, the true positive of the considered work is more than that of the other works. Besides, average frames per second obtained by this work is more than the average frames obtained by Töreyn’s and Ko’s methods. Therefore, performance of the fire detection process – which is applied in the proposed system – is better than that of most existing related works.

5. Circuit Design of the Quadcopter Side

The quadcopter is composed of various electromechanical devices to reach the predefined goals. Fig. 8 depicts the main electronic devices, especially sensors, of the circuit in the quadcopter side, which is designed and simulated in Proteus Pro 8.4 SP0 Build 21079. An ATmega32 microcontroller is used as the main controller to manage the input and output devices. All of the sensors are connected to the microcontroller via port A. LM35DZ temperature sensor is connected to pin 0, SHT11 humidity sensor is connected to pins 1 and 2, and a MQ-2 gas sensor is connected to pin 3.

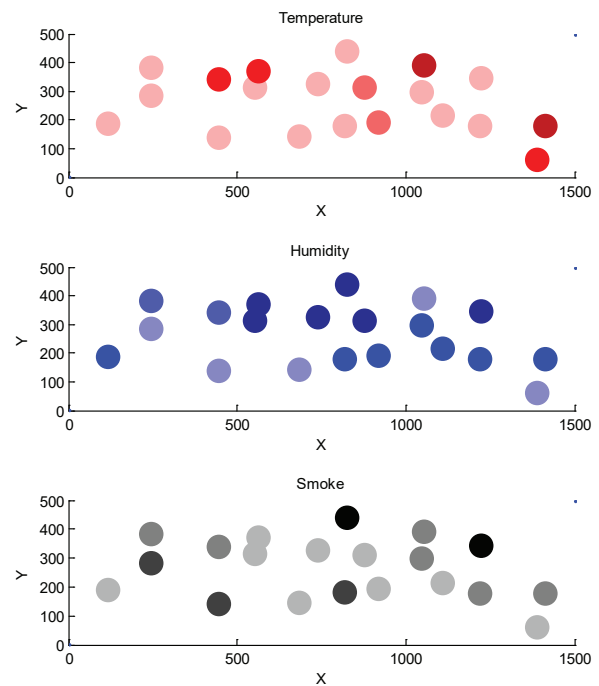


Fig. 7. Simulation results of the image processing unit in the temperature, humidity, and smoke monitors

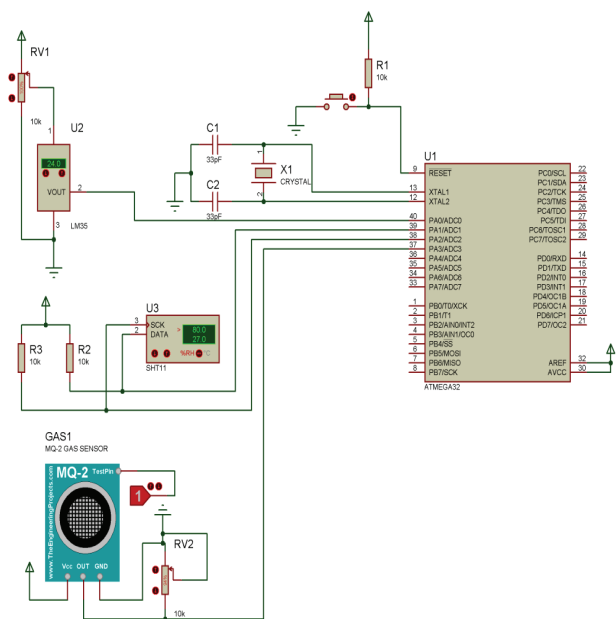


Fig. 8. Main electronic devices of the circuit in the quadcopter side

Table 4. Comparison results of the pattern recognition and Bayesian network unit in terms of true positive and detection speed [38]

Video sequence	True positive (Percentage)			Detection speed (Frames per second)		
	The considered work	Töreyn's method	Ko's method	The considered work	Töreyn's method	Ko's method
Movie 1	55	8	68	17.7	13.5	7.3
Movie 2	96	65	80	14.8	12.6	5.9
Movie 3	99	80	95	12.6	17.4	1.9
Movie 4	95	20	85	7.99	13.3	0.4
Movie 5	98	58	84	13	13.2	1.5
Movie 6	100	76	95	13.5	14	1.2
Movie 7	95	50	72	14.8	12.8	4.7
Movie 8	100	100	100	15.8	13.1	10.7
Movie 9	100	100	100	15.9	13.4	10.6
Movie 10	100	100	100	15.9	13.7	10.7
Movie 11	99	100	100	16	12.8	10.7
Movie 12	100	100	100	9.5	11.2	5.4
Average	95.3	72	88.6	14.0	13.4	5.9

6. Conclusions

A cloud-based urban monitoring system was proposed in this paper that uses a quadcopter and some of the intelligent learning systems. The quadcopter utilizes the temperature, humidity, and smoke sensors in addition to a camera and Global Positioning System (GPS) to transmit the phenomena data to a control station. All data are stored in a MongoDB cloud database to maintain all environmental conditions of the urban areas. This system is composed of several units including deep learning, fuzzy systems, and image processing, as well as

pattern recognition and Bayesian networks. The deep learning unit calculates climate status based on the sensing data of all the sensors. It uses a deep neural network to determine an appropriate status according to the pre-defined weights. The system controls four monitors to graphically illustrate conditions of the urban areas: climate monitor, temperature monitor, humidity monitor, and smoke monitor. The climate monitor is designed by a fuzzy system, image processing techniques, and RGB colors. The suggested fuzzy system consists of two inputs, namely “number of repeats” and “distance to mean”, as well as one output, namely “selection rate”. In contrast, the other monitors only use image processing techniques and RGB colors to show the temperature, humidity, and smoke data by means of graphical tools. Finally, the pattern recognition and Bayesian network unit detects the fire occurrence by using irregular patterns of flames and hierarchical Bayesian network.

Evaluation results were carried out based on the simulation results of deep learning, all the graphical monitors, as well as pattern recognition and Bayesian network. The results obtained by algorithm of the last unit are compared to some of the existing fire detection algorithms in terms of true positive and detection speed. Comparison results indicate that it has a high efficiency in most implemented cases. The main electronic circuit of the quadcopter side is designed and simulated in Proteus Pro 8.4 SP0 Build 21079.

AUTHORS

Sohrab Khanmohammadi – Faculty of Electrical and Computer Engineering, University of Tabriz, Tabriz, Iran

Mohammad Samadi* – Polytechnic Institute of Porto, Portugal, Email: mmasa@isep.ipp.pt

References

- [1] U. Lee, B. Zhou, M. Gerla, E. Magistretti, P. Bellavista, A. Corradi, “Mobeyes: smart mobs for urban monitoring with a vehicular sensor network,” *IEEE Wireless Communications*, vol. 13, no. 5, 2006, pp. 52–57. DOI: 10.1109/WC-M.2006.250358
- [2] P. J. Urban, G. Vall-Llosera, E. Medeiros, S. Dahlfort, “Fiber plant manager: An OTDR-and OTM-based PON monitoring system,” *IEEE Communications Magazine*, vol. 51, no. 2, 2013, pp. S9–S15. DOI: 10.1109/MCOM.2013.6461183
- [3] A. del Amo, A. Martínez-Gracia, A. A. Bayod-Rújula, J. Antoñanzas, “An innovative urban energy system constituted by a photovoltaic/thermal hybrid solar installation: Design, simulation and monitoring,” *Applied Energy*, vol. 186, 2017, pp. 140–51. DOI: 10.1016/j.apenergy.2016.07.011
- [4] I. Sa, P. Corke, “Vertical infrastructure inspection using a quadcopter and shared autonomy control,”

- Field and Service Robotics*. Springer, 2014, pp. 219–32. DOI: 10.1007/978-3-642-40686-7_15
- [5] X. Song, K. Mann, E. Allison, S.-C. Yoon, H. Hila, A. Muller, C. Gieder, “A quadcopter controlled by brain concentration and eye blink”, Proceedings of the IEEE Signal Processing in Medicine and Biology Symposium (SPMB), Philadelphia, PA, 3-3 Dec. 2016, pp. 1–4. DOI: 10.1109/SPMB.2016.7846875
- [6] D. E. Chang, Y. Eun, “Global Chartwise Feedback Linearization of the Quadcopter with a Thrust Positivity Preserving Dynamic Extension,” *IEEE Transactions on Automatic Control*, vol. 62, no. 9, 2017, pp. 4747–52.
- [7] C. Yang, Q. Huang, Z. Li, K. Liu, F. Hu, “Big Data and cloud computing: innovation opportunities and challenges,” *International Journal of Digital Earth*, vol. 10, no. 1, 2017, pp. 13–53.
- [8] M. Sookhak, A. Gani, M. K. Khan, R. Buyya, “Dynamic remote data auditing for securing big data storage in cloud computing,” *Information Sciences*, vol. 380, 2017, pp. 101–16. DOI: 10.1016/j.ins.2015.09.004
- [9] Y. Zhang, M. Qiu, C.-W. Tsai, M. M. Hassan, A. Alamri, “Health-CPS: Healthcare cyber-physical system assisted by cloud and big data,” *IEEE Systems Journal*, vol. 11, no. 1, 2017, pp. 88–95. DOI: 10.1109/JSYST.2015.2460747
- [10] J. L. Schnase, D. Q. Duffy, G. S. Tamkin, D. Nadeau, J. H. Thompson, C. M. Grieg, M. A. McNerney, W. P. Webster, “MERRA analytic services: meeting the big data challenges of climate science through cloud-enabled climate analytics-as-a-service,” *Computers, Environment and Urban Systems*, vol. 61, 2017, pp. 198–211. DOI: 10.1016/j.compenvurbsys.2013.12.003
- [11] Nakamura J., *Image sensors and signal processing for digital still cameras*, CRC Press, Boca Raton, 2016.
- [12] Y. LeCun, Y. Bengio, G. Hinton, “Deep learning”, *Nature*, vol. 521, no. 7553, 2015, pp. 436–44. DOI: 10.1038/nature14539
- [13] Goodfellow I., Bengio Y., Courville A., *Deep Learning*, MIT Press, 2016.
- [14] W. Samek, A. Binder, G. Montavon, S. Lapuschkin, K.-R. Müller, “Evaluating the visualization of what a deep neural network has learned,” *IEEE transactions on neural networks and learning systems*, vol. PP, no. 99, 2016, pp. 1–14. DOI: 10.1109/TNNLS.2016.2599820
- [15] F. J. Cabrerizo, F. Chiclana, R. Al-Hmouz, A. Morfeq, A. S. Balamash, E. Herrera-Viedma, “Fuzzy decision making and consensus: challenges,” *Journal of Intelligent & Fuzzy Systems*, vol. 29, no. 3, 2015, pp. 1109–1118. DOI: 10.3233/IFS-151719
- [16] N. A. Korenevskiy, “Application of fuzzy logic for decision-making in medical expert systems,” *Biomedical Engineering*, vol. 49, no. 1, 2015, pp. 46–49. DOI: 10.1007/s10527-015-9494-x
- [17] T. Runkler, S. Coupland, R. John, “Interval type-2 fuzzy decision making,” *International Journal of Approximate Reasoning*, vol. 80, 2017, pp. 217–224. DOI: 10.1016/j.ijar.2016.09.007
- [18] Z. Hao, Z. Xu, H. Zhao, R. Zhang, “Novel intuitionistic fuzzy decision making models in the framework of decision field theory,” *Information Fusion*, vol. 33, 2017, pp. 57–70. DOI: 10.1016/j.inffus.2016.05.001
- [19] Devroye L., Györfi L., Lugosi G., *A probabilistic theory of pattern recognition*, Springer Science & Business Media: Berlin, 2013, vol. 31.
- [20] C. Bielza, P. Larrañaga, “Discrete Bayesian network classifiers: a survey,” *ACM Computing Surveys (CSUR)*, vol. 47, no. 1, 2014, Article No. 5. DOI: 10.1145/2576868
- [21] F. Calabrese, M. Colonna, P. Lovisolo, D. Parata, C. Ratti, “Real-time urban monitoring using cell phones: A case study in Rome,” *IEEE Transactions on Intelligent Transportation Systems*, vol. 12, no. 1, 2011, pp. 141–151. DOI: 10.1109/TITS.2010.2074196
- [22] K. Abraham, S. Pandian, “A low-cost mobile urban environmental monitoring system,” Proceedings of the 4th IEEE International Conference on Intelligent Systems Modelling & Simulation (ISMS), Bangkok, Thailand, 29-31 Jan. 2013, pp. 659–664. DOI: 10.1109/ISMS.2013.76
- [23] J. Lee, Z. Zhong, B. Du, S. Gutesa, K. Kim, “Low-cost and energy-saving wireless sensor network for real-time urban mobility monitoring system,” *Journal of Sensors*, vol. 2015, 2015, pp. 1–8. DOI: 10.1155/2015/685786
- [24] K. B. Shaban, A. Kadri, E. Rezk, “Urban air pollution monitoring system with forecasting models,” *IEEE Sensors Journal*, vol. 16, no. 8, 2016, pp. 2598–2606. DOI: 10.1109/JSEN.2016.2514378
- [25] W. Zhao, T. H. Go, “Quadcopter formation flight control combining MPC and robust feedback linearization,” *Journal of the Franklin Institute*, vol. 351, no. 3, 2014, pp. 1335–1355. DOI: 10.1016/j.jfranklin.2013.10.021
- [26] J. Schmidhuber, “Deep learning in neural networks: An overview,” *Neural Networks*, vol. 61, 2015, pp. 85–117. DOI: 10.1016/j.neunet.2014.09.003
- [27] M. Havaei, A. Davy, D. Warde-Farley, A. Biard, A. Courville, Y. Bengio, C. Pal, P.-M. Jodoin, H. Larochelle, “Brain tumor segmentation with deep neu-

- ral networks," *Medical Image Analysis*, vol. 35, 2017, pp. 18–31. DOI: 10.1016/j.media.2016.05.004
- [28] C.-C. Hsu, K.-S. Wang, H.-Y. Chung, S.-H. Chang, "A study of visual behavior of multidimensional scaling for kernel perceptron algorithm," *Neural Computing and Applications*, vol. 26, no. 3, 2015, pp. 679–691. DOI: 10.1007/s00521-014-1746-2
- [29] Ross T. J., *Fuzzy logic with engineering applications*, John Wiley & Sons, 2009.
- [30] M. Cococcioni, L. Foschini, B. Lazzerini, F. Marceloni, "Complexity reduction of Mamdani Fuzzy Systems through multi-valued logic minimization," Proceedings of the IEEE International Conference on Systems, Man and Cybernetics, Singapore, 12–15 Oct. 2008, pp. 1782–1787. DOI: 10.1109/ICSMC.2008.4811547
- [31] M. S. Gharajeh, S. Khanmohammadi, "Dispatching Rescue and Support Teams to Events Using Ad Hoc Networks and Fuzzy Decision Making in Rescue Applications," *Journal of Control and Systems Engineering*, vol. 3, no. 1, 2015, pp. 35–50. DOI:10.18005/JCSE0301003
- [32] M. S. Gharajeh, S. Khanmohammadi, "DFRTP: Dynamic 3D Fuzzy Routing Based on Traffic Probability in Wireless Sensor Networks," *IET Wireless Sensor Systems*, vol. 6, no. 6, 2016, pp. 211–219. DOI: 10.1049/iet-wss.2015.0008
- [33] S. Khanmohammadi, M. S. Gharajeh, "A Routing Protocol for Data Transferring in Wireless Sensor Networks Using Predictive Fuzzy Inference System and Neural Node," *Ad Hoc & Sensor Wireless Networks*, vol. 38, no. 1–4, 2017, pp. 103–124.
- [34] M. S. Gharajeh, "FSB-System: A Detection System for Fire, Suffocation, and Burn Based on Fuzzy Decision Making, MCDM, and RGB Model in Wireless Sensor Networks," *Wireless Personal Communications*, vol. 105, no. 4, 2019, pp. 1171–1213. DOI: 10.1007/s11277-019-06141-3
- [35] M. S. Gharajeh, "Implementation of an Autonomous Intelligent Mobile Robot for Climate Purposes," *International Journal of Ad Hoc and Ubiquitous Computing*, vol. 31, no. 3, 2019, pp. 200–218. DOI: 10.1504/IJAHUC.2019.10022345
- [36] M. S. Gharajeh, "A Knowledge and Intelligence-based Strategy for Resource Discovery on IaaS Cloud Systems," *International Journal of Grid and Utility Computing*, vol. 12, no. 2, 2021, pp. 205–221. DOI: 10.1504/IJGUC.2021.114819
- [37] M. S. Gharajeh, H. B. Jond, "Speed Control for Leader-Follower Robot Formation Using Fuzzy System and Supervised Machine Learning," *Sensors*, vol. 21, no. 10, 2021, Article ID 3433. DOI: 10.3390/s21103433
- [38] B. C. Ko, K.-H. Cheong, J.-Y. Nam, "Early fire detection algorithm based on irregular patterns of flames and hierarchical Bayesian Networks," *Fire Safety Journal*, vol. 45, no. 4, 2010, pp. 262–270. DOI: 10.1016/j.firesaf.2010.04.001
- [39] B. U. Töreyn, Y. Dedeoğlu, U. Güdükbay, A. E. Cetin, "Computer vision based method for real-time fire and flame detection," *Pattern Recognition Letters*, vol. 27, no. 1, 2006, pp. 49–58. DOI: 10.1016/j.patrec.2005.06.015
- [40] B. C. Ko, K.-H. Cheong, J.-Y. Nam, "Fire detection based on vision sensor and support vector machines," *Fire Safety Journal*, vol. 44, no. 3, 2009, pp. 322–329. DOI: 10.1016/j.firesaf.2008.07.006